Geochemical Perspectives Letters

Magnesiowüstite as a major nitrogen reservoir in Earth´s lowermost mantle

G. Rustioni, M. Wiedenbeck, N. Miyajima, A. Chanyshev, H. Keppler

Supplementary Information

The Supplementary Information includes:

- Methods Supplementary Information
- Figures S-1 to S-4
- Tables S-1 and S-2

Methods Supplementary Information

Raman spectroscopy

Raman spectra were measured at Bayerisches Geoinstitut, Bayreuth using a confocal Horiba Labram 800 HR UV spectrometer with an 1800 mm^{-1} grating, a Peltier-cooled CCD detector, and a 50 x objective. Spectral resolution was about 3 cm^{-1}. The 514 nm line of an argon laser with 200 mW output power as used for excitation. Spectra were acquired with 2 x 5 s or 2 x 50 s accumulation time. The sensitivity of Raman spectrometry for the ammonium ion and other N-H species is demonstrated in Figure S-1.

Transmission electron microscopy (TEM)

TEM studies, combined with energy-dispersive X-ray spectroscopy (EDS, Bruker-Quantax system) and electron energy-loss spectroscopy (EELS, Gatan GIF Quantum SE), were carried out with a 200 kV FEI Titan G2 80-200 S/TEM instrument. TEM thin foils were prepared using a FEI Scios focused ion beam instrument. The foils were investigated by selected area electron diffraction and conventional bright-field and dark-field imaging in TEM mode. The ELNES (energy loss near edge structure) spectrum of a single-crystal area of N-rich magnesiowüstite was measured in a scanning TEM mode. The conditions were convergent semi-angle (alpha) 10 mrad, collection semi-angle (beta) 17 mrad, and 200 s integration time (2 s exposure x 100 times). Figures S-2, S-3, and S-4 show additional evidence for the homogeneous distribution of N in single crystals of magnesiowüstite. The EDS elemental maps (Fig. S-3) were acquired for 420 s with the same beam conditions in the scanning TEM mode. The resolution of the pixel size is 3 nm in the 256 x 256-pixel map.

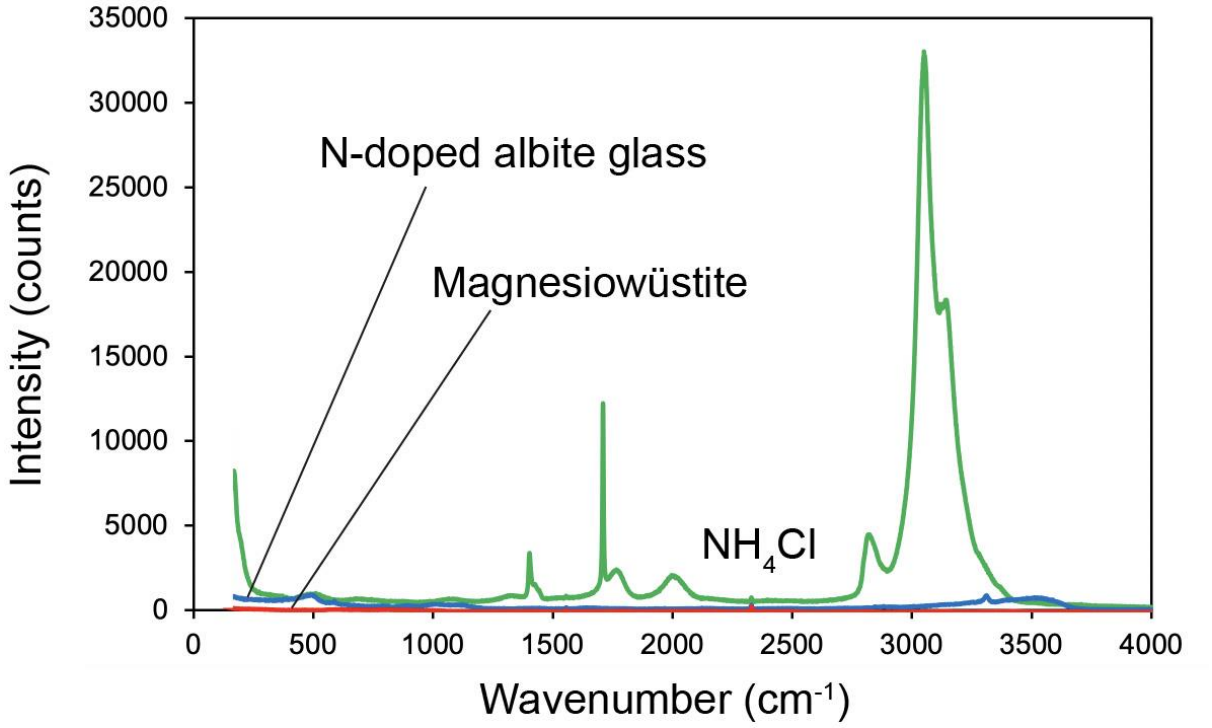

Figure S-1 A demonstration of the sensitivity of Raman spectroscopy for the ammonium ion and other N-H species. Raman spectra of pure NH_4Cl, a N-bearing hydrous albite glass with 0.8 wt. % of N and a N-rich magnesiowüstite sample were measured under the same conditions (2 times 5 s accumulation time, 200 mW output power, 514 nm Ar laser). Note that the accumulation time here is 10 times lower than for the spectra in Figure 3 of the main text, the magnesiowüstite and albite glass samples are the same. Nevertheless, even after 5 s, the N-H stretching band near 3300 cm^{-1} is still seen in the albite glass spectrum (see also Fig. 3 in the main text). The intensity roughly scales with the N-H stretching band system from 2800 – 3300 cm^{-1} in NH_4Cl as expected from the difference in nitrogen concentration.

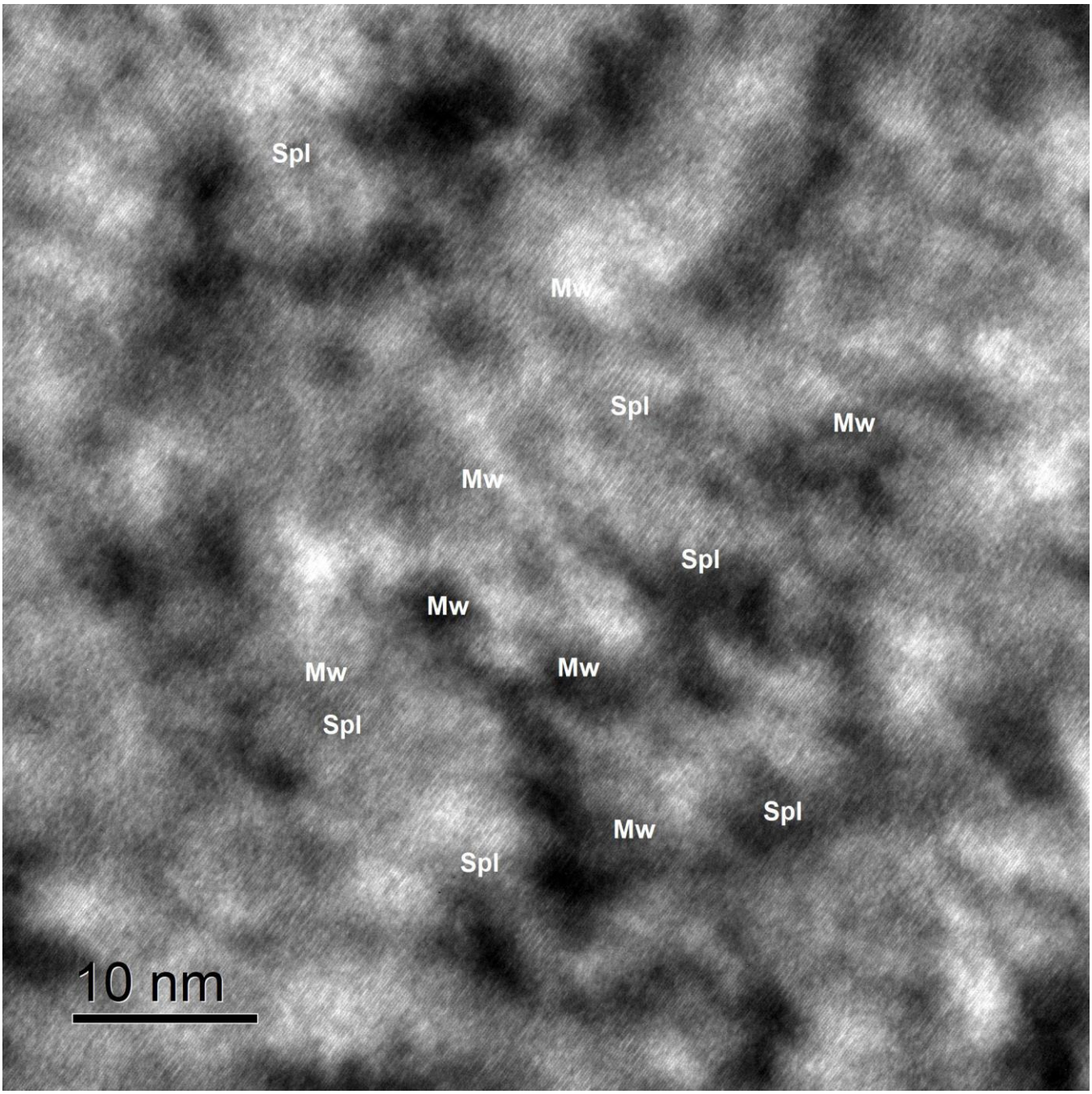

Figure S-2 High-resolution lattice TEM image of a single crystal of nitrogen-rich magnesiowüstite (Mw) with an exsolved spinel phase (Spl). The {220} fringes of 0.15 nm (Mw) and 0.30 nm (Spl) are visible. The image shows that no foreign N-bearing phases are present.

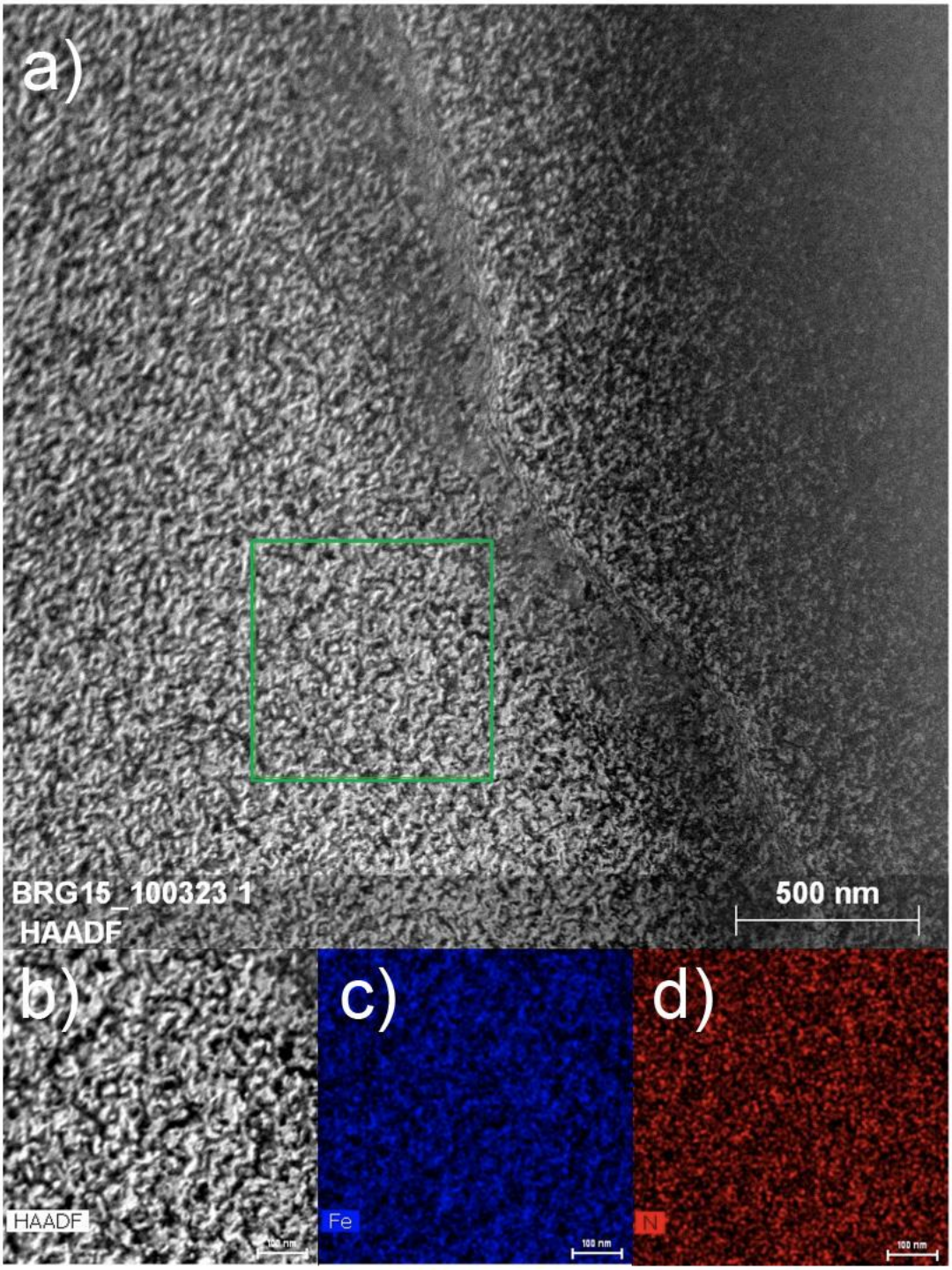

Figure S-3 **(a)** High-angle annular dark field (HAADF)-STEM image of a single crystal of N-rich magnesiowüstite. **(b)** The corresponding area (green square in the image a) of Fe and N elemental maps as seen by energy-dispersive X-ray spectroscopy (EDS; image **c and d**). Variations in local Fe-K and N-K X-ray intensity are within the range expected from counting statistics for a chemically homogeneous sample.

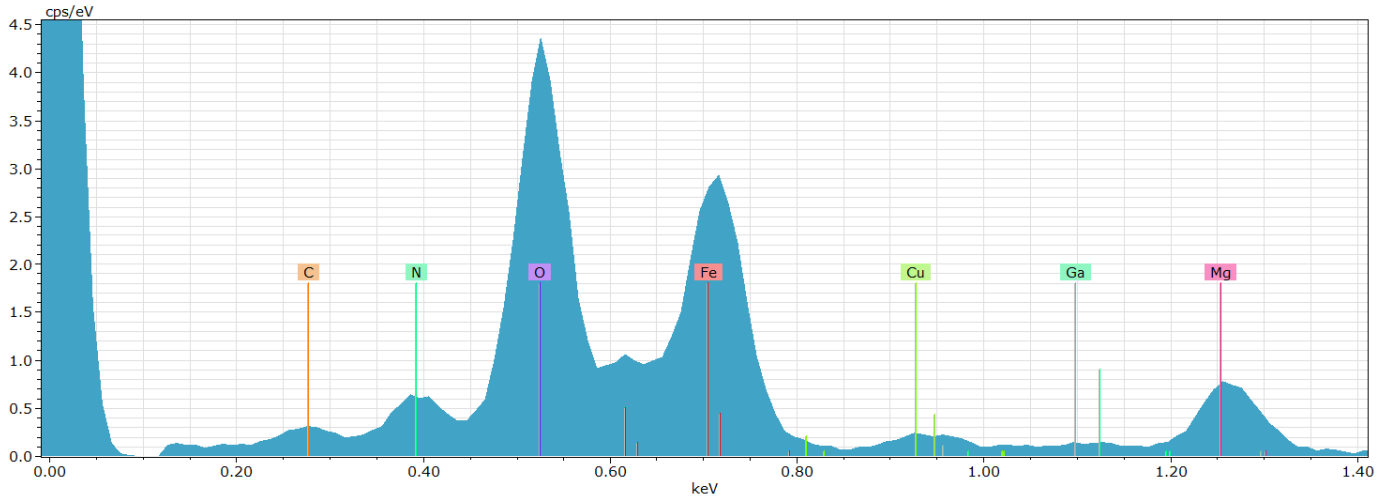

Figure S-4 A representative EDS spectrum (up to 1.4 keV) produced from part of the region shown in Figure S-3b. The peak of the N K-line is clearly detected.

Table S-1 Summary of high-pressure experiments on nitrogen solubility in ferropericlase - magnesiowüstite.

Run no	P (GPa)	T (˚C)	Duration (hrs)	Phases	Fe (wt. %) in metal	FeO (wt. %) in fp	N (wt. %) EPMA	N (wt. %) SIMS
MAJ01*	20	1700	5	maj, rw, fp, st, mtl	5.8 – 8.9	85.0 – 86.7	0.025 – 0.13	0.19 – 0.30
S7160	24	1600	1	br,fp, mtl	26.0 – 30.2	93.2 – 98.2	4.0 – 6.0	10.8
S7124	24	1600	3	br, fp, mtl	20.4 – 41.5	96.9 – 99.0	2.0 – 7.0	-
H4804	24	1600	3	br, fp, mtl	74.6 – 75.8	90.2	-	6.9
BRG01	24	1700	1.5	br, fp, st	4.9 – 12.7	89.1 – 93.5	0.11 – 0.42	-
BRG03*	24	1700	6	br, rw, fp, st	-	79.9	0.04 – 0.14	-
BRG05	24	1700	5.5	br, fp, st, mtl	6.6 – 8.8	80.6 – 83.4	-	1.3 – 1.4
BRG14*	24	1700	6.5	br, fp, st, mtl	3.3 – 9.1	85.0 – 89.5	0.066 – 0.28	-
BRG15	24	1700	6	br, fp, st, mtl	9.1 – 9.5	94.3 – 95.8	3.5 – 5.0	-
BRG21	24	1700	5	br, fp, mtl	97.8 – 98.6	83.7 – 100	0.17 – 18.1	0.2 – 2.3
BRG22	24	1700	6	br, fp, st, mtl	23.5 – 26.3	89.2 – 93.3	2.0 – 3.1	5.9 – 6.6
FPER01	24	1700	6	br, fp, mtl	75.9 – 90.1	26.8 – 97.7	< DL – 11.0	0.0014 – 0.063
BRG23	24	1800	6	br, fp, mtl	61.4 – 63.7	84.0 – 93.8	0.42 – 0.68	2.8
BRG24	24	1800	6	br, fp,mtl	12.6 – 13.0	85.3 – 91.3	2.6 – 4.1	-
IBRG01	33	1800	2	br, fp, st, mtl	41.0 – 42.1	93.7 – 98.6	1.2 – 4.3	6.5 – 14.0

EPMA (Electron microprobe) and SIMS (secondary ion mass spectrometry) measurements were not carried out at the same spot, because of the nitrogen loss associated with the measurements. In general, for each sample only one or two measurements were carried out by SIMS and about five by electron microprobe. FeO concentrations in the ferropericlase-magnesiowüstite solid solutions are microprobe data from the same spots as the nitrogen measurements. *Runs marked with a star contain either no metal phase at all or the metal phase is nearly pure Pt with little Fe, such that oxygen fugacity likely as not buffered near the Fe-FeO equilibrium; results from these three runs are therefore not plotted in Figure 2. Abbreviations: br = bridgmanite, fp = ferropericlase or magnesiowüstite, depending on FeO content, maj = majorite, rw = ringwoodite, st = stishovite, mtl = Fe-Pt metal alloy, DL = detection limit.

Table S-2 SIMS data on nitrogen solubility in ferropericlase - magnesiowüstite.

Sample	P	T (˚C)	SiO_2 (wt. %)	Al_2O_3 (wt. %)	MgO (wt. %)	FeO (wt. %)	Sum oxides (wt. %)	^{15}N (wt. %)
MAJ01_a	20	1700	0.91	0.34	7.83	85.94	95.02	0.30
MAJ01_b	20	1700	0.98	0.24	9.55	85.00	95.77	0.19
S7160	24	1600	0.05	0.05	5.13	94.30	99.5	10.77
H4804	24	1600	0.01	0.09	10.03	90.24	100.4	6.94
BRG05_a	24	1700	0.24	0.01	14.70	83.41	98.4	1.41
BRG05_b	24	1700	0.25	0.00	15.44	80.56	96.2	1.34
BRG21_a	24	1700	0.03	0.12	1.12	98.65	99.9	2.26
BRG21_b	24	1700	0.00	0.33	13.28	85.96	99.6	0.20
BRG22_a	24	1700	0.02	0.21	9.16	90.01	99.4	5.86
BRG22_b	24	1700	0.03	0.15	6.27	92.12	98.6	6.58
BRG23	24	1800	2.37	0.03	16.52	84.03	102.9	2.79
IBRG01_a	33	1800	0.00	0.33	3.05	93.86	97.2	6.48
IBRG01_b	33	1800	0.02	0.11	3.48	94.93	98.5	14.05
FPer01_a	24	1700	0.15	n.m.	24.91	75.29	100.3	0.063
FPer01_b	24	1700	0.16	n.m.	15.13	84.76	100.0	0.027
FPer01_c	24	1700	0.002	n.m.	66.69	33.66	100.3	0.0014
FPer01_d	24	1700	0.0271	n.m	56.76	43.5	100.3	0.0017

^{15}N concentrations were measured by SIMS (secondary ion mass spectrometry). The data shown are measurements from one single spot each, such that no meaningful standard deviation can be given. The major elements were measured by electron microprobe at a spot close to the SIMS measurement. n.m. = not measured.